

# PGE 383 Final Report - Team 01

Jayaram Hariharan, Preston Fussee-Durham, Jorge Navas, Ningjie Hu

## 1 Executive Summary

Reservoir Subsurface Team 1 has received delivery of 271 wells in a data table with X and Y coordinates (meters), Facies 0 and 1 (1 is sandstone and 0 is shale), Porosity (fraction), permeability as Perm (mD) and acoustic impedance as AI ( $\frac{kg}{m^2s} \cdot 10^6$ ) along with an acoustic impedance map with exhaustive coverage at 10 x 10m resolution over the 1 x 1km area of interest.

This information was used to inform subsurface modeling of the reservoir using geostatistical methods. Ultimately estimates about the total amount of oil present in this reservoir were made, with an assessment of the uncertainty surrounding the estimates. The work includes:

- Initial data processing and removal of outliers
- Removal of trends via Gaussian convolution
- Variogram modeling of spatial continuity
- Estimation of properties across the reservoir via kriging
- Simulation of the entire reservoir using indicator and gaussian simulation methods
- Quantification of the uncertainty in the simulations using bootstrap and Monte Carlo methods

Based on spatial simulation results, the P10, P50, and P90 of original oil in place was found to be 14.93, 16.36, and 17.65 million barrels. This represents an increase of 6.9% from previous estimates. Uncertainty in the geological interpretation regarding the depositional environment still remains and further analysis is needed. We currently believe the reservoir to contain both lobe-like and channel features. We propose the next well should be located at X = 540m and Y = 760m. The proposed location is consistently within a region of high porosity throughout all spatial estimations and simulations. This position was chosen by maximizing the expected porosity value while accounting for pre-existing, producing wells. Uncertainty quantification for porosity at the proposed well location suggests a non-gaussian, bimodal distribution with a mean of 0.161 and standard deviation of 0.019. Future analyses should incorporate dynamic measures for judging future well placement rather than the static porosity model used here.

## 2 Discussion and Results

The data from the 271 wells acquired is analyzed and applied to describe and characterize the reservoir. The subsequent sections describe these methods and processes as well as the significant findings and results.

## 2.1 Initial Data Processing - Outlier Removal

Of the initial 271 wells, 54 were identified via the Tukey method as being outliers (Figure 1b). These outliers had permeability values exceeding practical values (10-25 Darcys). In order to avoid biasing future results and analyses by including these extraordinarily high values, we drop these outliers and work with the remaining 217 samples to characterize the reservoir.

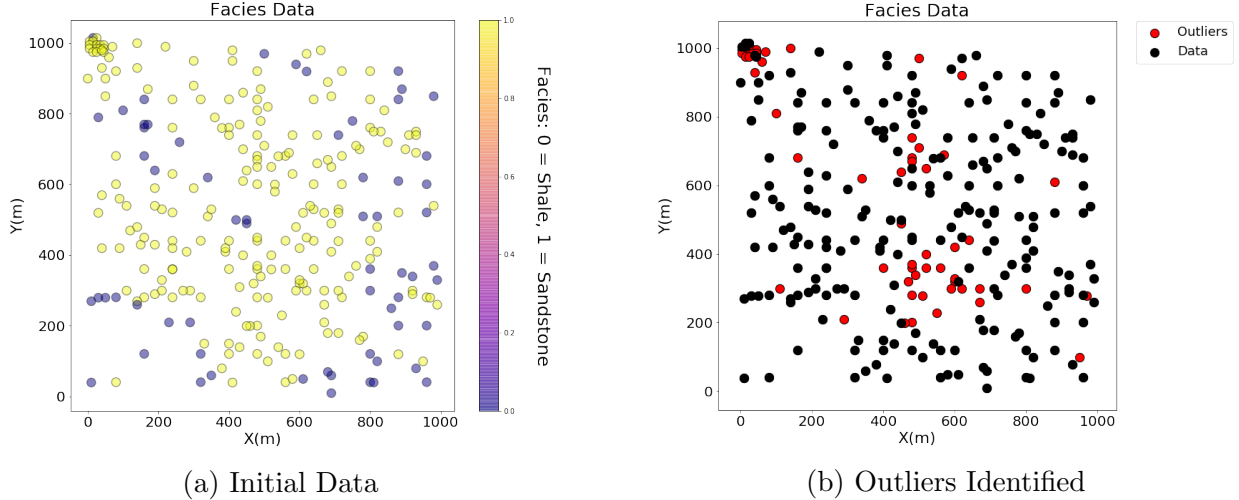


Figure 1: All Well Data and Outlier Identification/Removal

## 2.2 Trend Removal - Gaussian Convolution

Trends were identified and removed from the data via convolution of a Gaussian kernel. A lack of obvious trends in the data prompted the team to select large kernel sizes with broad standard deviations. The trend in porosity data was modeled using a kernel with a size of 410m and a standard deviation of 300m, this trend accounted for about 12% of the variance present in the data (Figure 2). A similar process was performed for the permeability data using a Gaussian kernel sized 510m with a standard deviation of 300m to model a trend representative of about 10% of the variance in the permeability data. Subsequent analysis is performed with the de-trended residuals.

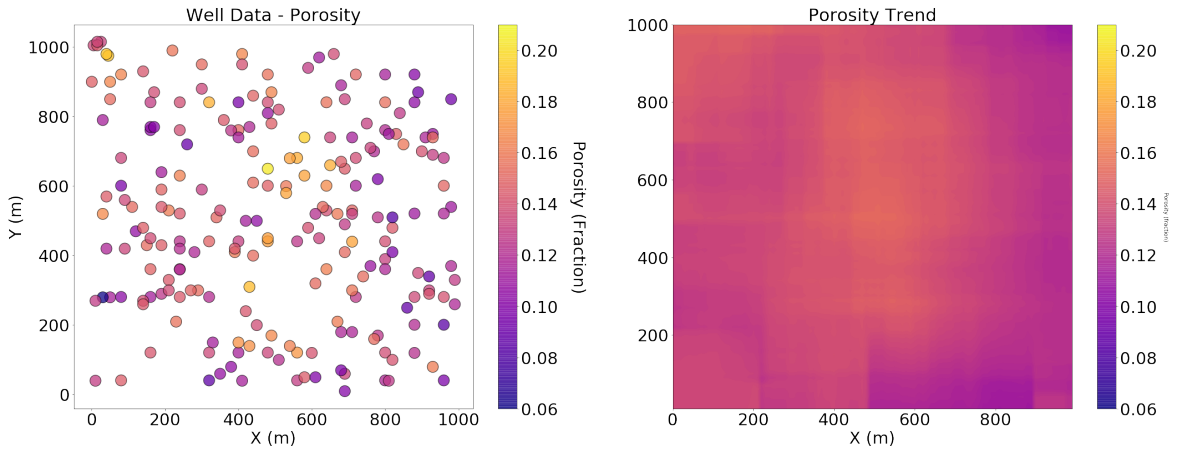


Figure 2: Porosity trend Modeling using a Gaussian Kernel

## 2.3 Spatial Continuity - Variogram Modeling

Variograms are experimentally calculated for different azimuthal directions. After identifying the major and minor directions from the experimental variograms, model variograms are fit to the data (Figure 3). This process is repeated for indicator transformed facies information, porosity, and permeability data (de-trended, by-facies) to determine major/minor directions and ranges of spatial continuity (Table 1).

Modeled Variograms - Major and Minor Directions and Ranges				
Property	Maj. Dir. (°)	Min. Dir. (°)	Maj. Range (m)	Min. Range (m)
Facies (Indicator)	112.5	202.5	500.0	250.0
Sandstone Porosity	45.0	135.0	170.0	70.0
Shale Porosity	0.0	90.0	150.0	5.0
Sandstone Perm.	67.5	157.5	300.0	20.0
Shale Perm.	0.0	90.0	600.0	250.0

Table 1: Summary of major/minor directions/ranges for variogram models of each property (by-facies)

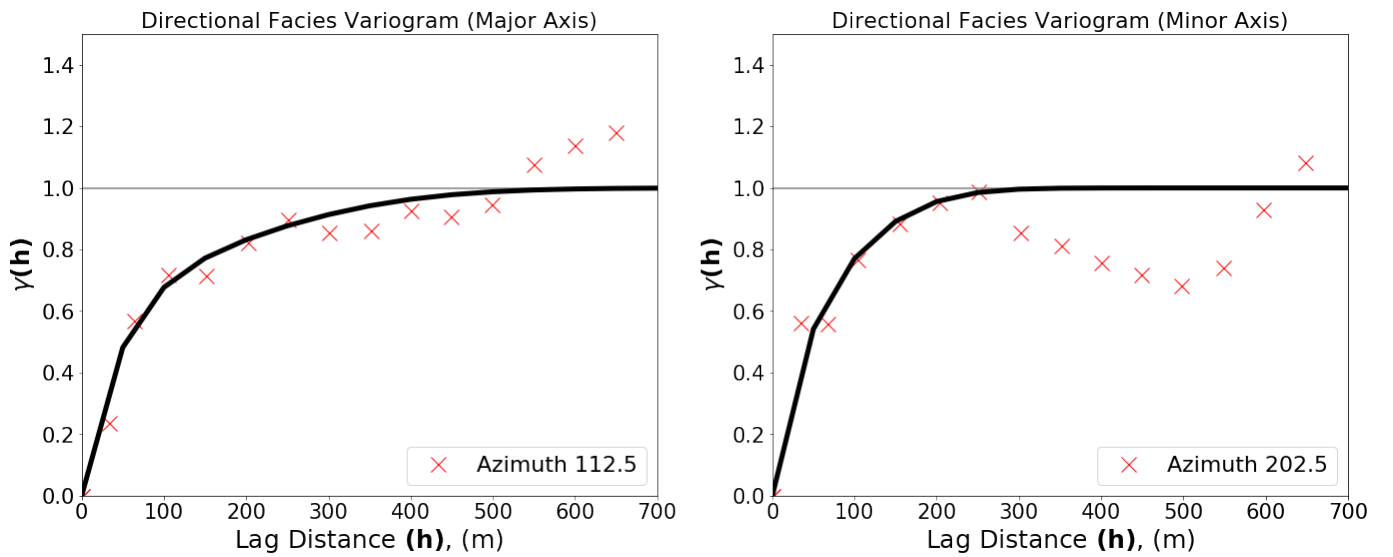


Figure 3: Modeled Indicator Variograms Overlaid on Experimental Indicator Variograms

## 2.4 Spatial Simulation

Sequential indicator simulation and sequential gaussian simulation are applied to estimate the distribution of spatial properties across the reservoir. These simulation methods are preferred over kriged maps as they capture the covariance between data points. A similar cookie-cutter approach is applied to combine the by-facies results into one map at the end of the simulations. The porosity values are estimated using sequential gaussian simulation, and using the relationship between porosity and permeability, collocated cokriging is used to perform sequential gaussian simulation and estimate the permeability values (Figure 4). These simulations are performed multiple times to resolve variability induced by the simulation method. For each simulation, output distributions are compared to the original distributions to ensure consistency (Figure 5).

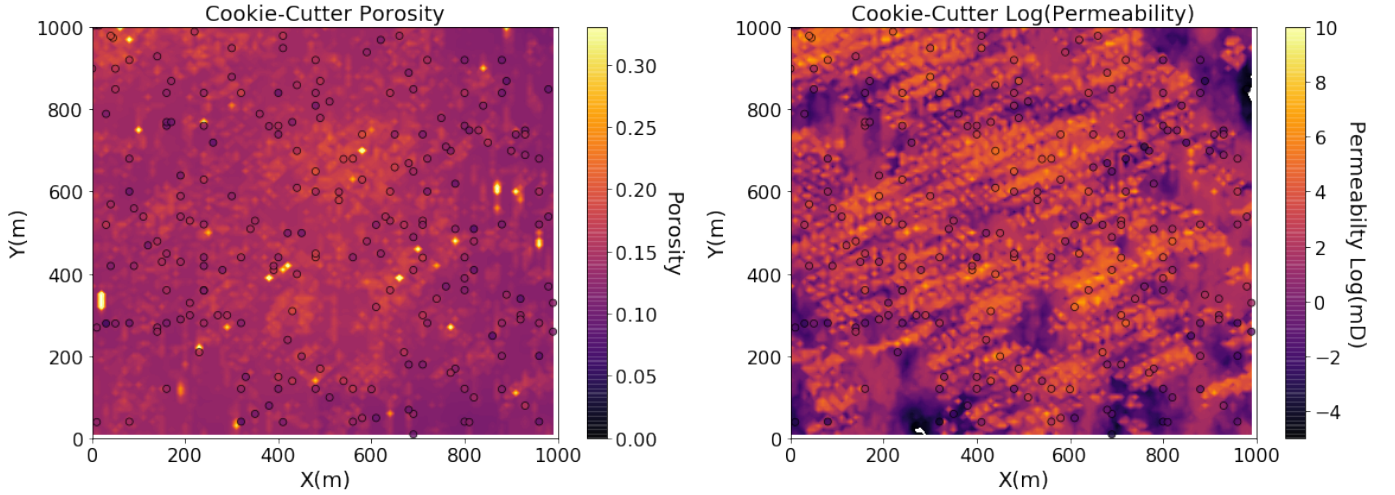


Figure 4: Example: Cookie-Cutter Simulation Results

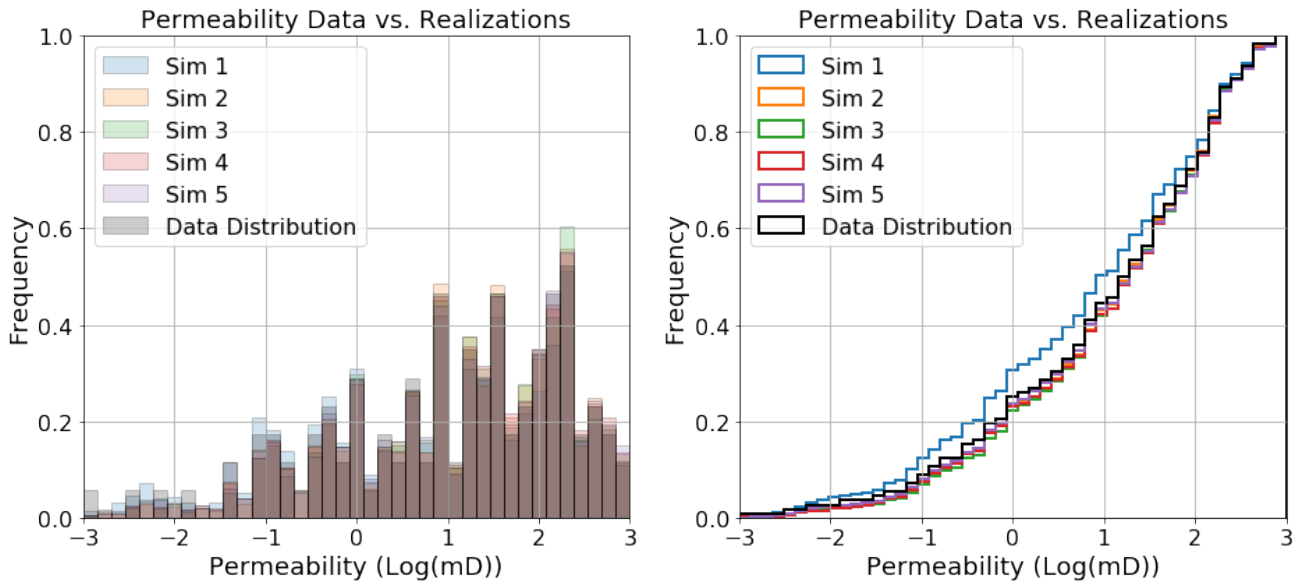


Figure 5: Comparison of Sample Permeability Distribution and Simulated Distributions

## 2.5 Uncertainty Quantification

Spatial bootstrap is applied to re-sample from the data distributions. The choice to use spatial bootstrap relative to ordinary bootstrap methods is to account for the effect of spatial correlation between samples. Based on the number of independent pieces of data (Table 2), sequential indicator simulation of facies and sequential Gaussian simulation of porosity values (by-facies) is performed 100 times. A cookie-cutter approach is used to combine sandstone porosity simulations and shale porosity simulations into a single map. Simulation results are used to produce an estimation of global oil in place (Figure 6) based on a reservoir thickness of 20.0 meters and saturation of 90%.

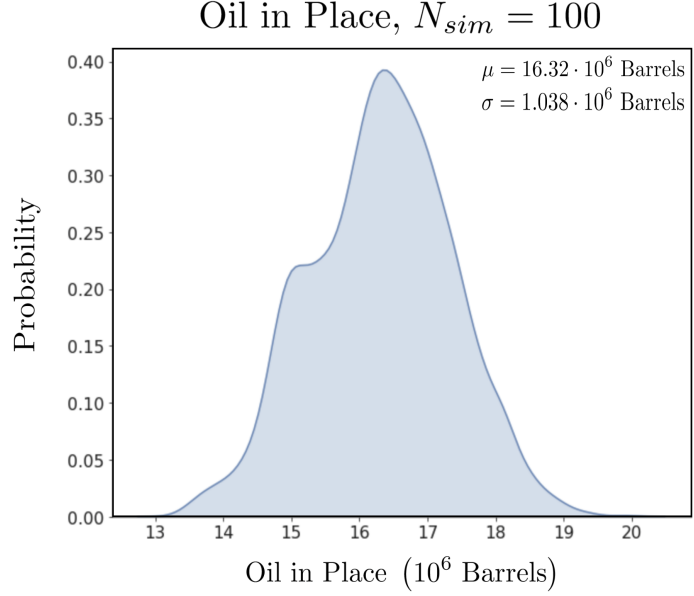


Figure 6: OIP based on an e-type model of 100 simulations.

Spatial Bootstrap Results		
Property	Number of Effective Samples	Total Number of Samples
Facies	20	217
Sandstone Porosity	91	164
Shale Porosity	42	53

Table 2: Effective number of samples used for simulations conducted to assess local uncertainty.

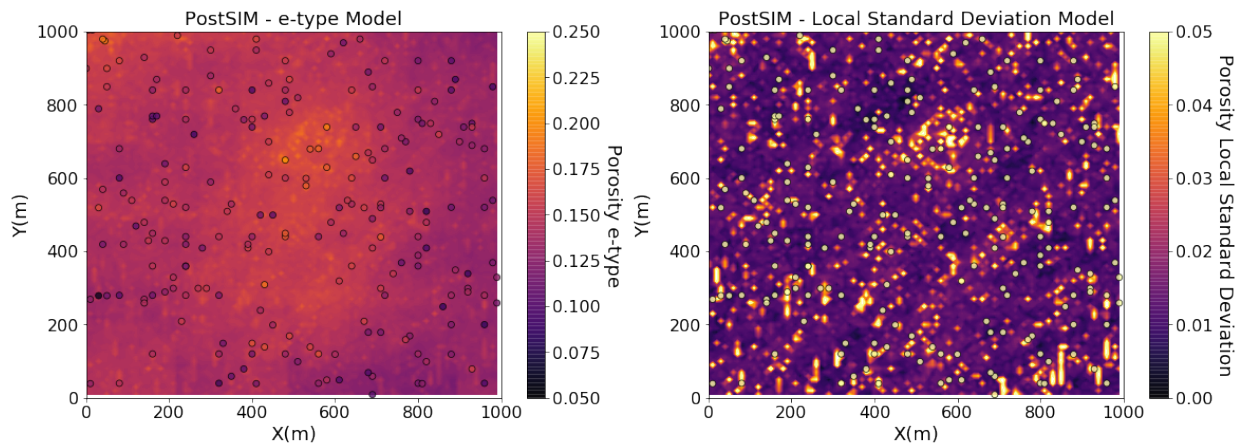


Figure 7: Local Expectation and Uncertainty (using 100 spatial bootstrapped sample simulations)

### 3 Future Development

We propose that the next well should be located at  $X = 540\text{m}$ , and  $Y = 760\text{m}$  (Figure 8, shown as the white '\*'). The position was chosen by maximizing the expected porosity value while accounting pre-existing, producing wells. The proposed location is consistently within a region of high porosity in all of the previous spatial estimations (Kriging, Simulation, Uncertainty Assessment), making it a good candidate for the next well.

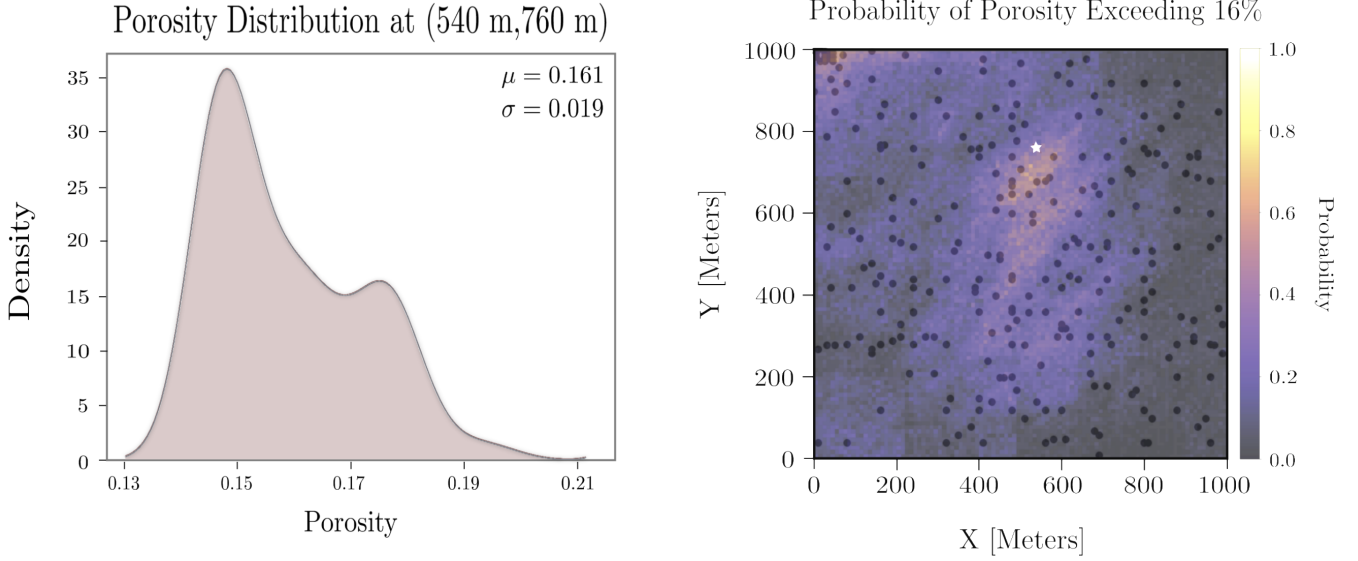


Figure 8: White star denotes the proposed Well Location (540 m, 760 m). Black dots indicate pre-existing wells. Left: KDE estimate of porosity distribution at proposed well location. Right: Exceedance map based on 100 Sequential Gaussian simulations (by-facies).

### 4 Srivastava Method

The Team No. 1 have decided to apply the Srivastava Method to the drainage area of the new well location. The goal of this application is the definition of the optimum amount of solvent to inject in the reservoir in order to avoid losses of inversion in this process of oil recovery. Initially, a drainage area was set of 100 m. In addition, an average oil price of 60 USD was taken. Then the ratio 10:1 was applied. 54 USD oil and 6 USD of solvent. Part of the process was the computation of OOIP in the new well area from the 100 porosity realizations similar to the previous updates. After the pro-

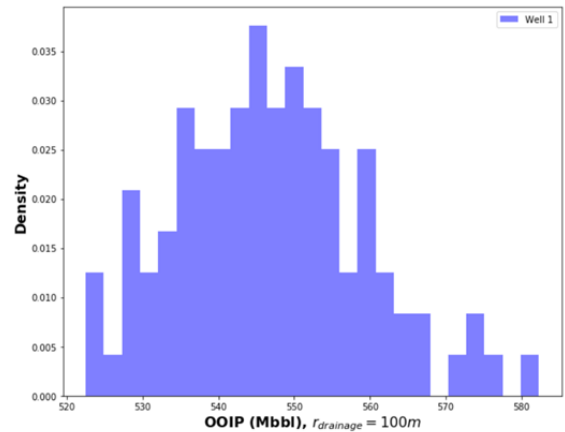


Figure 9: OOIP Distribution of the drainage area of the new proposed well (Mbbnl=  $10^3$  barrels)

cess mentioned above, the loss function was calculated, which quantifies the loss / cost of over- and underestimation. Additionally, we calculate the plot of expected loss as a function of estimate. From this plot we estimate the optimum amount of solvent to inject in the new well from an uncertainty distribution given a loss function. The optimum injected solvent volume is 562000 Bbls.

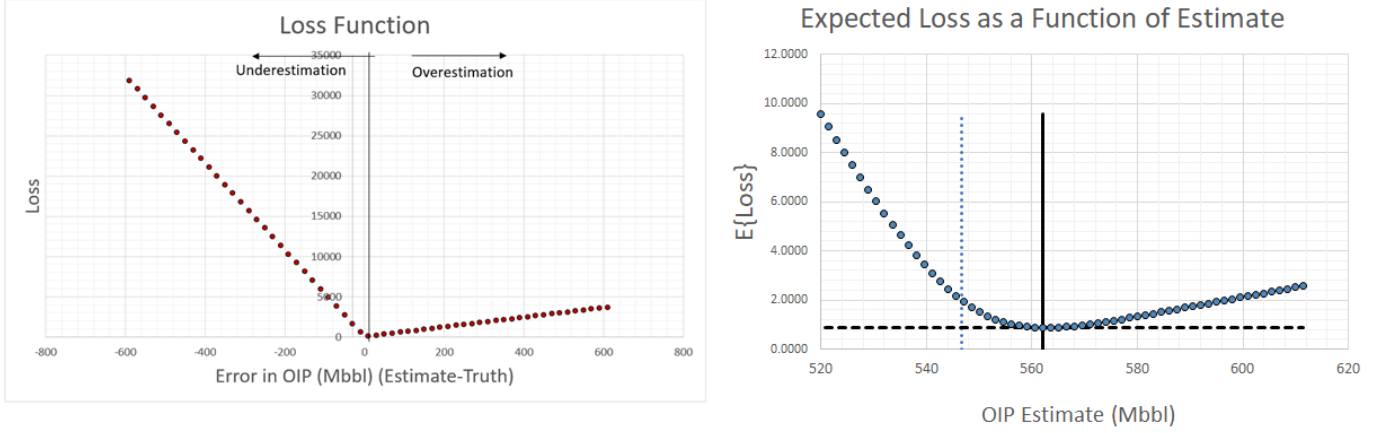


Figure 10: Loss Function and Expected Loss as a function estimate for the calculation of the optimum amount of solvent

## 5 Limitations and Proposed Improvements

The model results are currently limited to two-point geostatistical methods. To accurately capture geological structures, such as channel-like or lobe-like features, we propose extending the model to multi-point methods. Furthermore, field development plans were based on static measures such as the spatial distribution of OIP and rock porosity. These static measures are not ideal for assessing the future performance of a well and dynamic measures based on flow simulation should be used. Furthermore, we suggest implementing reservoir development optimization techniques to aide future development plans. In addition, this work is not including the saturation model. Water, Oil saturation and likely Gas saturation. The addition of this information to the permeability and porosity data will complement the petrophysical model. The delivered data set also does not include critical information such as pressure data or production history. These assumptions will significantly impact the location of the proposed well. We strongly encourage including key pressure information prior to finalizing future development plans.



## 6 Appendix

### 6.1 Description of Workflows and Methods

The following steps were conducted in an annotated Python Jupyter Notebook:

1. The raw data was analyzed for outliers
  - Tukey method of outlier removal was applied
2. Trend in the data was removed to make the field stationary
  - Convolution of Gaussian kernel was used to remove the trend
3. Spatial continuity was modeled
  - Directional variogram modeling identified major and minor directions and ranges of spatial continuity
4. Spatial estimation of the field
  - Using kriging and the cookie-cutter approach a kriged map was generated
  - Preliminary map with known deficiencies associated with kriging (over-smoothing)
5. Spatial simulation of the field
  - Cookie-cutter method applied to sequential indicator simulation and sequential Gaussian simulation of facies and rock properties
  - Multiple realizations with statistics and continuity more representative of the original data than kriged realizations
6. Uncertainty quantification
  - Applied spatial bootstrap to quantify uncertainty with consideration for spatial bias in data samples
  - Multiple realizations of multiple models performed to gauge uncertainty in reservoir estimates

### 6.2 Concepts

#### 6.2.1 Stationarity / Trend

A slight trend is identified in the reservoir and removed via the convolution of a Gaussian kernel. Once the trend is removed, we consider the field stationary at the scales over which we are interested.

#### 6.2.2 Scale

The reservoir area of interest is 1km x 1km, and we discretize this domain into 10,000 square 10m x 10m cells. This means that heterogeneity and phenomena occurring at scales smaller than 10m are not captured by this modeling approach.

#### 6.2.3 Statistics

Summary statistics as well as histograms and cumulative distribution plots were used throughout the reservoir modeling process to ensure that simulated models honored the original data. The Tukey method was applied to remove outliers.



#### **6.2.4 Hypothesis Testing**

Acoustic impedance data collected at wells was compared with the continuous seismic data. The null hypothesis,  $H_0 : \mu_{\text{Wells}} = \mu_{\text{Acoustic}}$ , could not be refuted when tested using the two sample t-test, rank-sum test, ANOVA test or the Kruskal-Wallace test.

#### **6.2.5 Confidence Intervals**

95% confidence bounds were used for all hypothesis testing.

#### **6.2.6 Spatial Estimation**

Indicator kriging was applied to estimate the spatial distribution of the facies. Ordinary kriging was applied on porosity and permeability data on a by-facies basis, and then the indicator kriging results were used to pick values from the most likely facies at each location to stitch together a cookie-cutter estimated realization.

#### **6.2.7 Spatial Simulation**

Sequential indicator simulation is used to simulate the distribution of facies across the reservoir. Sequential Gaussian simulation is applied to simulate spatial information. Information from porosity is leveraged using collocated cokriging to simulate the permeability of the reservoir.

#### **6.2.8 Uncertainty**

Uncertainty in estimates were initially quantified using the bootstrap method, and later refined using the spatial bootstrap.